I. PERTURBATIONS AFTER INFLATION

We've shown that inflation can generate fluctuations, and argued that curvature perturbations are constant once outside the horizon. We now need to study how they evolve after re-heating, when the universe contains matter and radiation, and fluctuations can gradually re-enter the horizon.

In principle this is straightforward: the Einstein equation

$$G_{\mu\nu} = \kappa T_{\mu\nu} = \kappa \sum_i T^{(i)}_{\mu\nu} \tag{1}$$

can be calculated for perturbed quantities, and relates the metric perturbations to the perturbed stress-energy tensor (density perturbations, peculiar velocities, etc). The sum on the right hand side sums over contributions to the stress-energy from photons, neutrinos, dark matter, baryons, dark energy, and any other components that may be present in the universe. To calculate how the different stress-energy components evolve we have to use the physics of the different components. This is not too complicated since neutrinos, dark matter and dark energy are assumed not to interact with anything else except indirectly via gravity. Electrons are very light and contribute very little to the energy density, but they scatter photons by Thomson scattering. They also interact very strongly electromagnetically with the positive charges (protons and Helium ions), and it's a good approximation to assume that the baryons and electrons therefore move around together. So before recombination the baryons are coupled to the photons via Thomson scattering of photons on electrons.

Conservation of stress-energy, ${T^{\mu\nu}}_{;\mu} = 0$ implies $\sum_i {T^{(i)\mu\nu}}_{;\mu} = 0$. If species do not interact they cannot exchange energy and momentum, so the stress energy of uninteracting species is separately conserved, ${T^{(j)\mu\nu}}_{;\mu} = 0$. Baryons and photons can exchange energy and momentum, but the total must of course be conserved.

For each species (or the total stress-energy) we decompose the perturbed stress-energy tensor as

$$\begin{aligned} {T^0}_0 &= \rho + \delta\rho & (2)\\ {T^i}_0 &= q^i = (\rho + P)v^i & (3)\\ {T^i}_j &= -(P + \delta P)\delta^i_j + \Pi_{ij} & (4) \end{aligned}$$

where i, j label spatial indices. $\delta\rho$ and δP are the density and pressure perturbations, v^i is the fluid velocity (q^i is the heat flux), and Π_{ij} the symmetric and trace-free anisotropic stress that we shall mostly neglect since it is zero for matter perturbations (and in inflation).

We shall assume the universe is spatially flat, $K = 0$, for simplicity, and work in the Conformal Newtonian Gauge with

$$ds^2 = a(\eta)^2[(1 + 2\Psi)d\eta^2 - (1 - 2\Phi)d\mathbf{x}^2]. \tag{5}$$

I will not give the detailed derivations of the result of substituting the metric into Einstein equations; personally I usually do things like this in Maple using GRTensor, where the tedious calculation of Christoffel symbols, Riemann and Einstein tensors can be automated. Most of the terms in the resulting equations have a clear physical significance, and can be related to familiar results in Newtonian gravity in the appropriate limit.

Newtonian limit

On small scales (with all velocities much lower than the speed of light, and hence $P \ll \rho$) we expect the full relativistic theory to recover standard Newtonian results in an expanding background. Of course even in Newtonian theory velocities change under a change of frame, so there is still some freedom in the choice of frame. However in Newtonian theory you can also unambiguously smooth the density over all space: choosing a frame at rest with respect to this averaged density is then the natural thing to do. Velocities with respect to this frame give the traditional Newtonian definition of the (peculiar) velocity. Alternatively one can use physical (non-comoving) spatial coordinates, in which case $\mathbf{r}_{\rm phys} = a\mathbf{x}$, so the Newtonian velocities $d\mathbf{r}_{\rm phys}/dt = H\mathbf{r}_{\rm phys} + ad\mathbf{x}/dt$ include the Hubble flow.

The Newtonian gauge is usually as close as you can get to simple Newtonian results in the relativistic theory[1]; for example in the Newtonian gauge observers will see a CMB without any dipole due to local velocity, a fairly natural alternative local definition of being 'at rest' with respect to the background. The Newtonian gauge has zero shear, meaning the local expansion rate is isotropic.

As we discussed in the section on cosmological perturbation theory, density perturbation modes on sub-horizon scales ($k \gg \mathcal{H}$) the difference under a change of gauge is negligible: for density perturbations well inside the horizon there are no gauge ambiguities, as we'd expect in a Newtonian universe. Gauge issues only become important on scales where the light travel time between points is comparable to the Hubble time, i.e. so that the background evolves significantly in the difference between the proper times of observers moving with different velocities.

A. Equations from conservation of stress-energy

We shall write all the equations in terms of conformal time, and denote derivatives with a dash, $X' \equiv \partial_\eta X$. The equation $T^{0\mu}{}_{;\mu} = 0$ gives the background result

$$\rho' = -3\mathcal{H}(\rho + P), \tag{6}$$

expressing conservation of energy, $(a^3\rho)' = -P(a^3)'$, i.e. the change in energy in a comoving volume is just the work PdV done. Extracting the first-order terms from $T^{0\mu}{}_{;\mu} = 0$ gives the corresponding equation for the perturbations

$$\delta\rho' = -3\mathcal{H}(\delta\rho + \delta P) - \boldsymbol{\nabla}\cdot\mathbf{q} + 3\Phi'(\rho + P). \tag{7}$$

The first term on the RHS is just the dilution due to the background expansion (as in the background equation), the $\boldsymbol{\nabla}\cdot\mathbf{q}$ accounts for the local fluid flow due to peculiar velocity, and the Φ' term is a purely relativistic effect corresponding to the density changes caused by perturbations to the local expansion rate [$(1-\Phi)a$ is the local scale factor in the spatial part of the CNG metric]. The equation can also be re-written for a density contrast $\Delta \equiv \delta\rho/\rho$:

$$\Delta' + (1+w)(\boldsymbol{\nabla}\cdot\mathbf{v} - 3\Phi') + 3\mathcal{H}\left(\frac{\delta P}{\rho} - w\Delta\right) = 0, \tag{8}$$

where $w = P/\rho$ and we substituted for ρ' using the background equation. This is sometimes called the continuity equation.

Turning to the equation $T^{i\mu}{}_{;\mu} = 0$ gives the linear equation

$$\mathbf{q}' + 4\mathcal{H}\mathbf{q} + (\rho + P)\boldsymbol{\nabla}\Psi + \boldsymbol{\nabla}\delta P + \text{anisotropic stress term} = 0. \tag{9}$$

We will neglect the anisotropic stress. Substituting $\mathbf{q} = (\rho + P)\mathbf{v}$ then gives the relativistic Euler equation for the velocity

$$\mathbf{v}' + \mathcal{H}\mathbf{v} + \frac{P'}{\rho + P}\mathbf{v} + \frac{\boldsymbol{\nabla}\delta P}{\rho + P} + \boldsymbol{\nabla}\Psi = 0. \tag{10}$$

The $\mathcal{H}$ term is just the effect of redshifting velocities, $\boldsymbol{\nabla}\Psi$ is the gravitational acceleration. These equations apply for the total matter and velocity, and *also separately* for any non-interacting components so that the individual stress-energy tensors are individually conserved.

It is useful to define the sound speed $c_s^2 \equiv \delta P/\delta\rho$, which is zero for dark matter but can be important for baryons which have some pressure that's important in small-scale perturbations. If $P = P(\rho)$ then $c_s^2 = \dot{P}/\dot{\rho} = P'/\rho'$.

---

[1] Actually as we shall see the Poisson equation in the full theory involves the Newtonian gauge potential, but the comoving-gauge density perturbation. So it is actually a combination of quantities in different gauges that gives most Newtonian results, e.g. as used when evolving numerical N-body simulations of the matter evolution. Specifically Newtonian calculations are effectively using the density perturbation is the comoving-gauge and velocities in the Newtonian gauge, which for matter is consistent with the full GR results (to leading orders) even on scales larger than the horizon.

1. Matter perturbations on sub-horizon scales

For matter perturbations we take $P_m \ll \rho_m$ so $w_m \approx 0$, and after recombination the baryons are no longer significantly coupled to the photons so the matter perturbations evolve independently. The dark matter perturbations always evolve independently. On sub-horizon scales $k/\mathcal{H} \gg 1$ and we can neglect Φ' compared to $\boldsymbol{\nabla}\cdot\mathbf{v}$ and also neglect $(\mathcal{H}\delta P)'$ compared to $\boldsymbol{\nabla}^2\delta P$. Then

$$\Delta_m' + \boldsymbol{\nabla}\cdot\mathbf{v}_m = 0 \tag{11}$$

$$\mathbf{v}_m' + \mathcal{H}\mathbf{v}_m + \boldsymbol{\nabla}(c_s^2\Delta_m) = -\boldsymbol{\nabla}\Psi. \tag{12}$$

The first equation is just the conservation of matter: the density only changes due to divergence in the flow. The second equation says that the acceleration is determined by the gravitational force and gradients in the pressure, with damping due to redshifting of the velocities. These are exactly the equations that one would get in linearised Newtonian gravity. Taking the divergence of the second equation and substituting into the first gives

$$\Delta_m'' + \mathcal{H}\Delta_m' - \boldsymbol{\nabla}^2(c_s^2\Delta_m) = \boldsymbol{\nabla}^2\Psi. \tag{13}$$

This shows that perturbations in each uninteracting matter species are driven by the gravitational potential Ψ. As we shall see, the RHS is simply determined from the total density perturbation by the Poisson equation.

B. Einstein equations

The equation $G_{00} = \kappa T_{00}$ (where $\kappa \equiv 8\pi G$) yields the Friedmann equation at lowest order

$$\mathcal{H}^2 = \frac{\kappa}{3}a^2\rho \tag{14}$$

and the first order equation

$$\boldsymbol{\nabla}^2\Phi - 3\mathcal{H}\Phi' = \frac{\kappa}{2}a^2\delta\rho + \kappa a^2\rho\Psi. \tag{15}$$

Note that in this section equations only hold for the *total* density, density perturbation and velocity, since these are what couple directly to gravity.

The $G_{0i} = \kappa T_{0i}$ equation gives

$$-\boldsymbol{\nabla}\Phi' - \mathcal{H}\boldsymbol{\nabla}\Psi = \frac{\kappa}{2}a^2\mathbf{q}. \tag{16}$$

We can then take the divergence of the G_{0i} equation and assuming zero boundary conditions invert to give

$$\Phi' + \mathcal{H}\Psi = -\frac{\kappa}{2}a^2(\rho+P)\boldsymbol{\nabla}^{-2}(\boldsymbol{\nabla}\cdot\mathbf{v}). \tag{17}$$

$$\implies \quad 3\mathcal{H}\Phi' + \kappa a^2\rho\Psi = -\frac{3\kappa}{2}a^2\mathcal{H}(\rho+P)\boldsymbol{\nabla}^{-2}(\boldsymbol{\nabla}\cdot\mathbf{v}) \tag{18}$$

where in the second line we used the Friedmann equation. Substituting into the G_{00} equation (15) then gives

$$\boldsymbol{\nabla}^2\Phi = \frac{\kappa}{2}a^2\left[\delta\rho - 3\mathcal{H}(\rho+P)\boldsymbol{\nabla}^{-2}(\boldsymbol{\nabla}\cdot\mathbf{v})\right]. \tag{19}$$

The term in the square brackets is the comoving density perturbation we derived before: the density perturbation in the comoving frame in which $v = 0$ so there is no peculiar velocity. The relativistic Poisson equation can therefore be written in terms of the comoving density perturbation $\bar{\delta\rho}$ as

$$\boldsymbol{\nabla}^2\Phi = \frac{\kappa}{2}a^2\bar{\delta\rho}. \tag{20}$$

We can relate Φ and Ψ by looking at an off-diagonal spatial part of the Einstein equation, e.g. the $G_{12} = \kappa T_{12}$ equation gives

$$\partial_x \partial_y (\Psi - \Phi) = 0 \tag{21}$$

in the absence of anisotropic stress. With suitable boundary assumptions, this implies $\Psi = \Phi$. Finally looking at the diagonal spatial parts of the Einstein equations, e.g. $G_{11} = \kappa T_{11}$ and using $\Psi = \Phi$ and the background equations gives

$$2\Phi'' + 6\mathcal{H}\Phi' - 6w\mathcal{H}^2\Phi = 3\mathcal{H}^2 \frac{\delta P}{\rho}. \tag{22}$$

II. GROWTH OF DENSITY PERTURBATIONS

1. *Sub-horizon matter perturbations ($k \gg \mathcal{H}$)*

We can now re-write the gravitational potential driving the evolution of the matter perturbations on sub-horizon scales from Eq. (13) using the Poisson equation. For cold dark matter $c_s^2 \sim 0$ but for baryons c_s can be important on small scales, so

$$\Delta_c'' + \mathcal{H}\Delta_c' = \frac{\kappa}{2} a^2 \bar{\delta\rho} = \frac{\kappa}{2} a^2 \sum_i \rho_{(i)} \bar{\Delta}_{(i)} \tag{23}$$

$$\Delta_b'' + \mathcal{H}\Delta_b' - \boldsymbol{\nabla}^2 (c_{s,b}^2 \Delta_b) = \frac{\kappa}{2} a^2 \bar{\delta\rho} = \frac{\kappa}{2} a^2 \sum_i \rho_{(i)} \bar{\Delta}_{(i)}. \tag{24}$$

In harmonic space $\boldsymbol{\nabla}^2 (c_{s,b}^2 \Delta_b) \to -k^2 c_{s,b}^2 \Delta_b$. On scales where $k c_{s,b} \ll \mathcal{H}$ this term is negligible and baryons and dark matter satisfy the same equation, and so does the total matter perturbation.

In the late universe, well after matter-radiation equality so radiation perturbations can be neglected, we can also write an equation for the total matter density $\rho_m = \rho_c + \rho_b$ which also obeys an energy conservation equation. From Eq. (13) and the Poisson equation, with $k \gg \mathcal{H}$ so gauge is not important and $\bar{\delta\rho} = \delta\rho = \delta\rho_m = \rho_m \Delta_m = \Omega_m(\eta)\rho\Delta_m$, using the Friedmann equation we then have

$$\Delta_m'' + \mathcal{H}\Delta_m' - \boldsymbol{\nabla}^2 (c_s^2 \Delta_m) - \frac{3}{2}\mathcal{H}^2 \Omega_m(\eta) \Delta_m = 0. \tag{25}$$

Ex: Show that this equation is consistent with Eqs. (23) and (24), with $\rho_m \Delta_m = \rho_b \Delta_b + \rho_c \Delta_c$ and $\rho_m = \rho_b + \rho_c$.

This shows that matter perturbation growth can be determined entirely from the background geometry which defines $\Omega_m(\eta)$ and $\mathcal{H}$ is the sound speed (due to baryon pressure) can be neglected. Note also that for $k \ll \mathcal{H}/c_s$ there is no scale (k) dependence, so perturbations on all scales with $\mathcal{H} \ll k \ll \mathcal{H}/c_s$ grow the same way.

2. *Matter domination ($k \gg \mathcal{H}$)*

Let's now keep the sound speed term and consider matter domination, with

$$\Delta_m'' + \mathcal{H}\Delta_m' + (k^2 c_s^2 - \frac{3}{2}\mathcal{H}^2)\Delta_m = 0, \tag{26}$$

or for the baryons

$$\Delta_b'' + \mathcal{H}\Delta_b' + k^2 c_{s,b}^2 \Delta_b - \frac{3}{2}\mathcal{H}^2 \Delta_m = 0. \tag{27}$$

The character of the baryon perturbation evolution therefore changes when $k^2 c_{s,b}^2 \Delta_b > 3\mathcal{H}^2\Delta_m/2$, corresponding to small enough scales that pressure support can resist gravitational collapse. After matter radiation equality as we shall see $\Delta_b \sim \Delta_m$ at late times, so to the characteristic wavenumber where pressure becomes important is $k \sim \sqrt{3/2}\mathcal{H}/c_{s,b}$. Writing $k = 2\pi/\lambda$ we can define the proper Jeans' length

$$\lambda_J = a\lambda = c_{s,b}\sqrt{\frac{\pi}{G\rho}} \tag{28}$$

corresponding to the smallest-sized baryonic structure that can collapse. Below this scale we expect the baryon and dark matter perturbations to behave differently: the baryon gas is pressure-supported, but the dark matter fluctuations grow roughly the same as on larger scales (assuming $\rho_b \ll \rho_c$).

On scales much larger than the Jeans' length we can neglect the $k^2 c_s^2$ term giving as before

$$\Delta_m'' + \mathcal{H}\Delta_m' - \frac{3}{2}\mathcal{H}^2\Delta_m = 0. \tag{29}$$

Substituting for $a \propto \eta^2$ during matter domination gives

$$\Delta_m'' + \frac{2}{\eta}\Delta_m' - \frac{6}{\eta^2}\Delta_m = 0, \tag{30}$$

with a decaying solution $\Delta \propto 1/\eta^3$ that we can ignore, and the growing solution $\Delta \propto \eta^2 \propto a$. So matter perturbations grow $\propto a$ on scales larger than the Jeans' length during matter domination. Note that the Poisson equation gives $k^2\Phi = -a^2\rho\Delta = \text{const}$, so the potential is constant even though the density perturbations are growing. This reflects the fact that though the density peaks grow $\propto a$, the physical size of the perturbation is stretched $\propto a$, so the potential $\sim GM/r$ remains constant.

Ex: Show what happens to matter perturbations larger than the Jeans length during cosmological constant (Λ) domination. What happens to the potentials?

3. Density perturbations during radiation domination $k \gg \mathcal{H}$

Radiation has $P = \rho/3$ and $\delta P = \delta\rho/3$, so $c_s^2 = 1/3$. The two stress-energy conservation equations on sub-horizon scales become

$$\Delta' + \frac{4}{3}\boldsymbol{\nabla}\cdot\mathbf{v} = 0 \tag{31}$$

$$\mathbf{v}' + \frac{1}{4}\boldsymbol{\nabla}\Delta + \boldsymbol{\nabla}\Psi = 0. \tag{32}$$

Note that the velocity of the radiation doesn't decay due to the Hubble expansion; this is because *momentum* is conserved and redshifts, but for a radiation fluid this comes purely from the $1/a$ redshifting of the energy per particle, so the bulk fluid velocities do not also redshift.

The two equations can then be combined to give the second-order equation

$$\Delta'' - \frac{1}{3}\boldsymbol{\nabla}^2\Delta = \frac{4}{3}\boldsymbol{\nabla}^2\Psi = \frac{2}{3}\kappa a^2\bar{\delta\rho} = 2\mathcal{H}^2\bar{\Delta}. \tag{33}$$

In harmonic space, for $k \gg \mathcal{H}$ we can neglect the RHS compared to $k^2\Delta$ and have

$$\Delta'' + \frac{k^2}{3}\Delta = 0 \tag{34}$$

corresponding to oscillatory solutions $\Delta \propto \sin(k\eta/\sqrt{3} + \alpha)$. These are called *acoustic oscillations*, and happen as an initial gravitational collapse is stopped by the high pressure of the radiation fluid, bounces back out, falls back in, and so on. For radiation the Jeans' length is comparable to the

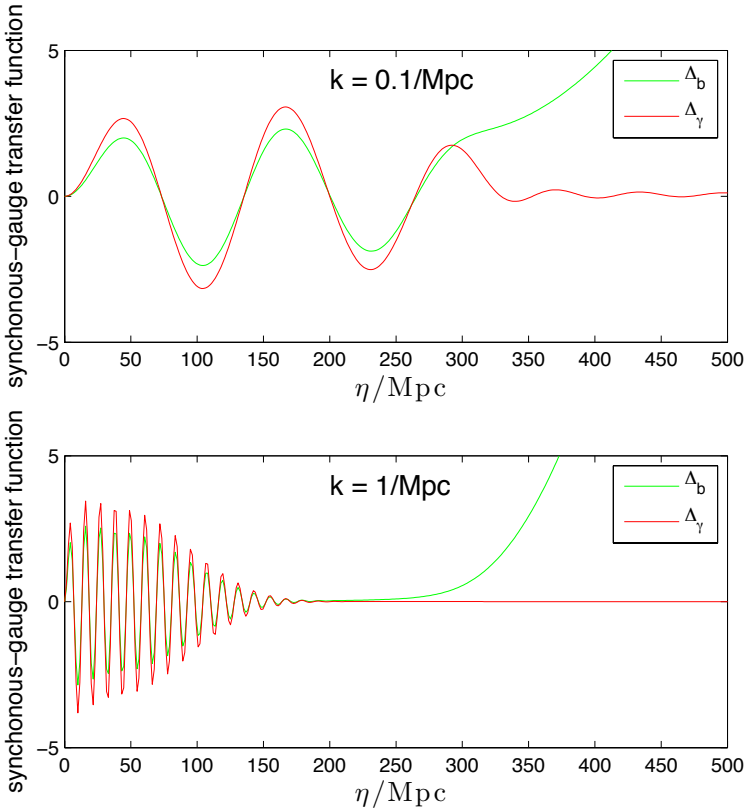

FIG. 1: Numerical evolution of adiabatic baryon and photon perturbation transfer functions for modes with two different wavenumber k. Both modes enter the horizon during radiation domination and undergo acoustic oscillations. The baryons follow the photons ($\Delta_b = \delta_b/\rho_b = \delta_\gamma/(\rho_\gamma + P_\gamma) = 3\Delta_\gamma/4$) because they are tightly coupled until around recombination (which is at $\eta_* \sim 270$Mpc). After recombination the baryons falls into the dark matter potential wells, and the perturbations grow. The smaller-scale mode in the lower panel also has significant Silk-damping (Sec. III 10): both oscillations are nearly completely damped out by the time of recombination due to photon diffusion.

horizon since the speed of sound is $1/\sqrt{3}$ the speed of light; perturbations below this scale oscillate. At recombination, $\eta = \eta_*$ we have $\Delta_* \propto \sin(k\eta_*/\sqrt{3} + \alpha)$, which oscillates in k. We shall see later how this leads to peaks in the observed spectrum of cosmic microwave background anisotropies.

For adiabatic perturbations initially $\Delta_\gamma = \Delta_\nu = \Delta$, and this will remain true until dynamical effects like free streaming become important (see later), or radiation domination ceases to be a good approximation. Also note that since the baryons are tightly coupled to the photons by Thomson scattering prior to recombination, during radiation domination the baryon perturbations will follow the dominant photon perturbations $\Delta_b \approx \Delta_\gamma$, and hence also undergo acoustic oscillations.

4. Dark matter perturbations during radiation domination ($k \gg \mathcal{H}$)

During radiation domination the matter perturbations are a sub-dominant component. As we have seen, on scales well below the radiation Jeans' length the dominant radiation perturbation oscillates rather than growing, $\Delta \propto \sin(k\eta/\sqrt{3} + \alpha)$. We can find the corresponding potential from the Poisson equation $\boldsymbol{\nabla}^2\Phi = \kappa a^2 \rho\bar{\Delta}/2 = 3\mathcal{H}^2\bar{\Delta}/2$. Since the amplitude of Δ is nearly constant once sub-horizon oscillations start, and in radiation domination $a \propto \eta$ so that $\mathcal{H} = 1/\eta$, Φ rapidly becomes very small. Pressure of the radiation fluid is preventing the perturbations growing significantly, so as the universe expands the physical size of the perturbations gets larger $\propto \eta \propto a$, and the corresponding gravitational potentials $\propto M/r$ become small, approximately zero.

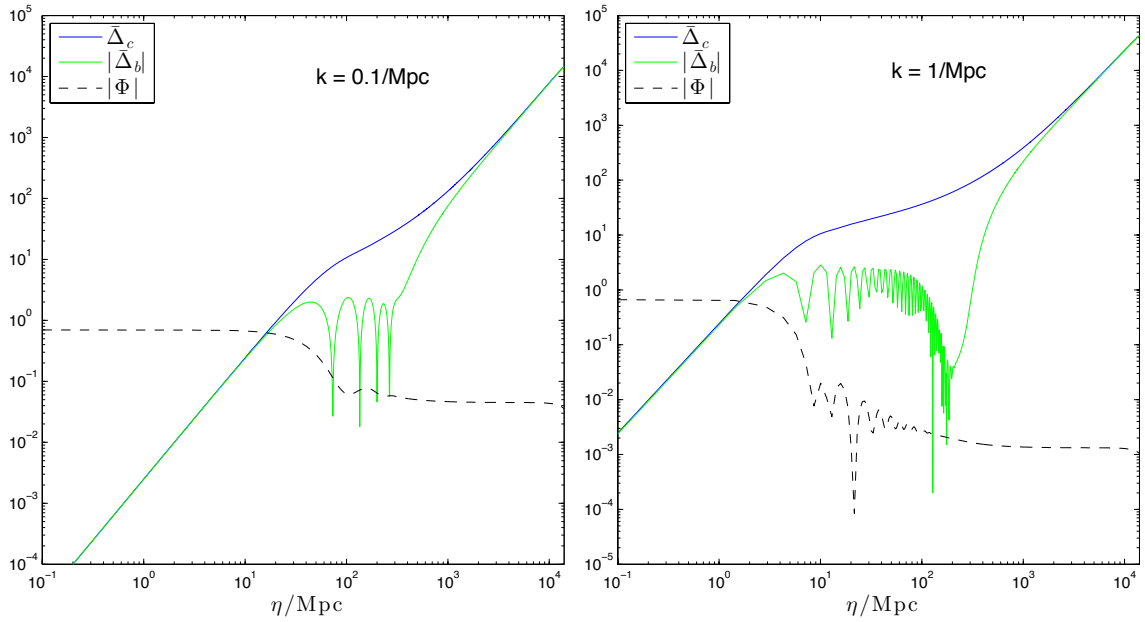

FIG. 2: Numerical evolution of the potential Φ and the comoving baryon and dark matter adiabatic perturbation transfer functions on a log scale (the absolute value of Δ_b is plotted where it undergoing acoustic oscillation and goes negative). The comoving dark matter perturbation initially grows, but once the mode enters the horizon photon-pressure support starts to prevents perturbation growth and the driving potentials become small: the dark matter perturbations then grow only logarithmically for $k\eta \gg 1$ until matter domination, as the dark matter particles continue slowly following their initial infall trajectories. The baryons undergo acoustic oscillations while coupled to the photons, but after recombination are free to fall into the dark matter potential wells. At late times during matter domination $\Delta_b \sim \Delta_c$ and both grow $\propto a$; the potential Φ is then constant until dark energy starts to be important. *[Note: spikes towards zero in the right plot are just a numerical artefact of plotting* $\ln(|\Delta|)$ *where* Δ *is sampled and crosses zero.]*

Using $\Psi \sim \Phi \sim 0$ in Eq. (13) with $\mathcal{H} = 1/\eta$, the dark matter perturbations therefore evolve with

$$\Delta_c'' + \frac{1}{\eta}\Delta_c' \sim 0 \tag{35}$$

with solution $\Delta_c = A + B\ln(\eta)$. This logarithmic growth in the dark matter perturbations on small scales $\propto \ln(a)$ is called the *Meszaros effect*.

The logarithmic growth is easy to understand. After the radiation perturbations start oscillating because of the high supporting pressure they stop growing. The gravitational potentials fall to zero as the physical size of the perturbations expand. After a while the dark matter then has no forces acting on it at all, so the velocities just redshift as $1/a \propto 1/\eta$. Since $\Delta_c' = -kv \propto 1/\eta$ we have $\Delta_c \sim \log(\eta)$. The log growth is just the growth due to infall velocities already built up when the driving potentials became small. See Fig. 2.

5. *Baryons in matter domination ($k \gg \mathcal{H}$)*

Prior to recombination the baryons are coupled to the photons, which are nearly smooth on small scales because the radiation pressure causes oscillations rather than growth, and because photons diffusion leads to very small scale fluctuations being wiped out (see later). Let's see what happens if we start matter domination with $\Delta_c \neq \Delta_b$. The equations well above the Jeans length ($c_s k \ll \mathcal{H}$ in matter domination)

$$\Delta_b'' + \mathcal{H}\Delta_b' = \frac{\kappa}{2}a^2\left(\rho_b\Delta_b + \rho_c\Delta_c\right) \tag{36}$$

$$\Delta_c'' + \mathcal{H}\Delta_c' = \frac{\kappa}{2}a^2\left(\rho_b\Delta_b + \rho_c\Delta_c\right). \tag{37}$$

Subtracting the equations we get

$$\Delta_{bc}'' + \mathcal{H}\Delta_{bc}' = 0 \tag{38}$$

where $\Delta_{bc} \equiv \Delta_b - \Delta_c$. So there is a solution $\Delta_{bc} = \text{const}$ and $\Delta_{bc}' = 1/a$. In matter domination $\mathcal{H} = 2/\eta$ and the solutions are $\Delta_{bc} = \text{const}$ and $\Delta_{bc} \propto 1/\eta$. Since Δ_m grows as $a \propto \eta^2$ in matter domination, $\Delta_{bc}/\Delta_m \propto 1/\eta^2$ and at late times we have $\Delta_c \sim \Delta_b \sim \Delta_m$. So well after recombination (so the baryons are no longer tightly coupled to the photons) it is a reasonable approximation to assume $\Delta_b \sim \Delta_c$ above the Jeans' length scale.

It is also interesting to look at the effect of the initial baryon distribution on the final matter distribution. Since we know from Eq. (25) that $\Delta_m \propto \eta^2$ even if $\Delta_c \neq \Delta_m$, at late times we must have

$$\Delta_c = \Delta_b = \Delta_m = \Delta_m^*\frac{\eta^2}{\eta_*^2} = (f_b\Delta_b^* + f_c\Delta_c^*)\frac{\eta^2}{\eta_*^2}, \tag{39}$$

where the baryon and CDM mass fractions are $f_b = \rho_b/(\rho_b + \rho_c)$, $f_c = \rho_c/(\rho_b + \rho_c)$. So the late-time matter perturbations are sensitive to structures in Δ_b at recombination. In particular the baryon-photon fluid at recombination has acoustic oscillations in k on scales inside the horizon, leading to Δ_b^* having a wiggly k-dependence. This leads to *baryon oscillations* in the late-time matter fluctuations, even though the initial dark matter perturbations were smooth in k. The wiggles in the total matter perturbation at late times are suppressed by f_b (and disappear on very small scales due to Silk damping; see Sec. III 10).

Below the Jeans' length scale the analysis is more complicated, and in detail requires knowing the time-dependence of c_s as the equation is then

$$\Delta_b'' + \mathcal{H}\Delta_b' + k^2c_s^2\Delta_b = \frac{3}{2}\mathcal{H}^2\Delta_m. \tag{40}$$

For $k^2c_s^2 \gg \mathcal{H}^2$ and the matter dominated by dark matter we can expect $\Delta_b \sim 3\Delta_c\mathcal{H}^2/(2k^2c_s^2)$, so the baryon perturbations are strongly suppressed on small scales where the baryon pressure is important.

6. Including super-horizon scales

We want to match the predictions from inflation to the perturbations at the beginning of the hot big bang, when all relevant scales are outside the horizon, so we now need to generalize previous results to be valid in the super-horizon regime.

On sub-horizon scales $\Delta \sim \bar{\Delta}$, but on super-horizon scales the difference can be important, and also potential terms that we dropped might be important, so we need to be a bit more careful. Let's consider the case of matter or radiation domination when $w = P/\rho$ is a constant (0 and 1/3 respectively) and $c_s^2 = w$. We shall be interested in the perturbation in the dominant component, so $\kappa a^2\rho\Delta = 3\mathcal{H}^2\Delta$. In harmonic space the Poisson equation, Eq. (19), is

$$-k^2\Phi = \frac{\kappa}{2}a^2\rho\bar{\Delta} = \frac{3}{2}\mathcal{H}^2\left[\Delta + 3\mathcal{H}(1+w)v/k\right]. \tag{41}$$

Using $\Psi = \Phi$ (no anisotropic stress), in harmonic space Eq. (17) becomes

$$\frac{3}{2}\frac{\mathcal{H}v}{k}(1+w) = \Phi + \frac{\Phi'}{\mathcal{H}}. \tag{42}$$

Inserting into the Poisson equation then gives

$$-k^2\Phi = \frac{3}{2}\mathcal{H}^2\bar{\Delta} = \frac{3}{2}\mathcal{H}^2[\Delta + 2\Phi + 2\Phi'/\mathcal{H}]. \tag{43}$$

Now we use Eq. (22) with $\delta P = c_s^2 \rho\Delta = w\rho\Delta$ to give

$$2\Phi'' + 6\Phi'\mathcal{H} - 3\mathcal{H}^2 w(\Delta + 2\Phi) = 0, \tag{44}$$

and substituting from Eq. (43) finally gives an equation for the potential:

$$\Phi'' + 3(1+w)\mathcal{H}\Phi' + k^2 w\Phi = 0. \tag{45}$$

In matter domination $w = 0$, so we can generalize the previous solution $\Phi = \text{const}$ to all scales.

7. *Super-horizon evolution ($k \ll \mathcal{H}$) and initial conditions*

More generally in the super-horizon limit $k \ll \mathcal{H}$ the last term in Eq. (45) can be dropped, so there is always a solution $\Phi = \text{const}$ on super-horizon scales (plus a decaying solution): super-horizon potentials are conserved once the decaying contribution can be neglected[2]. Using a super-horizon constant Φ in Eq. (43) gives

$$\bar{\Delta} = -\frac{2}{3}\frac{k^2}{\mathcal{H}^2}\Phi = \Delta + 2\Phi. \tag{46}$$

This means that the comoving density perturbation for $k \ll \mathcal{H}$ is initial very small ($\bar{\Delta} \propto k^2/\mathcal{H}^2$), but the Newtonian gauge $\Delta = -2\Phi$, which is a constant (to $\mathcal{O}(k\eta)^2$ corrections). So the large-scale behaviour of the density perturbation is completely different in the different gauges:

$$\text{Newtonian gauge} \ : \ \Delta = -2\Phi = \text{const} \tag{47}$$

$$\text{Comoving gauge} \ : \ \bar{\Delta} = -\frac{2}{3}\frac{k^2}{\mathcal{H}^2}\Phi \propto (k\eta)^2. \tag{48}$$

In both matter and radiation domination $\mathcal{H} \propto 1/\eta$, so $\bar{\Delta} \propto (k\eta)^2$. In matter domination $a \propto \eta^2$, so the comoving perturbation grows as $\bar{\Delta} \propto a$, in radiation domination $a \propto \eta$, so it grows as $\bar{\Delta} \propto a^2$. In both cases the Newtonian gauge density perturbation and the potential are a constant, with $\Delta = -2\Phi$. The Newtonian gauge velocity $v \propto 1/\mathcal{H} \propto \eta$.

If the comoving curvature perturbation at the start of the hot big bang is $\mathcal{R}$, the initial super-horizon conditions in radiation domination give (using the general gauge-invariant definition of $\mathcal{R}$), $\mathcal{R} = -\Phi + \Delta/4 = -3\Phi(0)/2$: in radiation domination the constant curvature perturbation and potential are just proportional, as you'd expect for perturbations with only one degree of freedom (adiabatic).

8. *Entering the horizon in radiation domination*

Perturbations all start outside the horizon during radiation domination, where $w = 1/3$. Using $w = 1/3$ in Eq. (45) we can find an equation valid for any $k/\mathcal{H}$ in radiation domination that can be used to studying perturbations entering the horizon:

$$\Phi'' + 4\mathcal{H}\Phi' + \frac{k^2}{3}\Phi = 0 \quad \Longrightarrow \quad \Phi'' + \frac{4}{\eta}\Phi' + \frac{k^2}{3}\Phi = 0. \tag{49}$$

Assuming no decaying modes at the start of the hot big bang – as expected for constant super-horizon $\mathcal{R}$ from inflation — the potential Φ is initially constant, $\Phi'(0) = 0$, and the solution is

$$\Phi = 3\frac{\sin(x) - x\cos(x)}{x^3}\Phi(0) \tag{50}$$

---

[2] If w changes, e.g. between radiation and matter domination, the potential can evolve due to decaying mode contributions in the in-between region: it doesn't have to be the *same* constant in matter and radiation domination, though actually it turns out to be quite close. The potential changes again once dark energy starts to become important.

where $x \equiv k\eta/\sqrt{3}$. As expected this starts off constant, and then falls off $\propto 1/\eta^2$ with acoustic oscillations once radiation pressure stops perturbation growth. The time at which $\Phi = \Phi(0)/2$ is roughly $\eta_{\rm ln} \sim 3\sqrt{3}\pi/(4k)$, which is roughly the time at which the growth of dark matter perturbations changes to being only logarithmic (Sec. II 4).

In terms of the density perturbation we can now generalize our previous sub-horizon acoustic-oscillation solution to

$$\bar{\Delta} = -\frac{2}{3}\frac{k^2}{\mathcal{H}^2}\Phi = -\frac{2}{3}(k\eta)^2\Phi = -2x^2\Phi = 4\left(\frac{\sin(x)}{x} - \cos(x)\right)\mathcal{R}, \tag{51}$$

where $\mathcal{R}$ is the random initial super-horizon curvature perturbation from inflation and the x-dependent pre-factor is the transfer function describing how the perturbation evolves forward in time. For small x (super-horizon scales) we have $\bar{\Delta} \propto (k\eta)^2$ as before, and for large x (sub-horizon scales) acoustic oscillations $\bar{\Delta} = 4\cos(k\eta/\sqrt{3})\mathcal{R}$. We have now solved for the arbitrary phase α that we didn't know when studying only sub-horizon perturbations in Sec. II 3, and have also related the amplitude to the $\mathcal{R}$ produced by inflation.

For adiabatic perturbations the densities are all perturbed in the same way (see inflation notes), so the super-horizon perturbations in each species in fact evolve the same way as the total. In general of course the universe is neither totally matter or radiation dominated, and the full equations should be integrated numerically. In particular Φ is not constant if w is not constant, though the change between radiation and matter domination turns out to be rather small (you can calculate it analytically using the constancy of $\mathcal{R}$ when anisotropic stress is neglected).

9. Summary so far

At the beginning of the hot big bang, all relevant scales are outside the horizon. Their potentials remain constant until they enter the horizon (assuming the perturbations enter the horizon during radiation domination). After horizon entry the radiation density perturbations oscillate because of the high radiation pressure. However the dark matter perturbations grow logarithmically. In matter domination the sub-horizon density perturbations grow $\propto a$ on all scales larger than the Jeans' length. Potentials remain constant during matter domination on all scales above the Jeans' length.

III. FREE STREAMING AND SILK DAMPING

So far we have taken the matter content of the universe to be an ideal fluid, so the only relevant quantities at a given point are the density, pressure and bulk velocity. This is a good approximation if the fluid is strongly interacting. However if the particles making up the fluid are less tightly coupled, individual fluid particles can travel a significant distance leading to dissipative diffusion effects. In particular, as the universe approaches recombination the scattering between photons and baryons becomes less effective, and photons can diffuse between hot and cold regions, leading to an averaging out of small-scale perturbations. Although the baryon particles move slowly, because they are still relatively tightly coupled to the photons the smoothing in the photons feeds back into a smoothing of the baryons. The perfect fluid approximation is only valid on scales much larger than the diffusion length (determined by the mean free path of particles and how many collisions they've random walked between collisions if they interact).

The term *free streaming* is sometimes applied to the free propagation of particles. At a given point in space, it is no longer just the density, pressure and velocity that is important, but the full angular distribution of the particles. The density is proportional the monopole of the angular distribution (total number of particles), and the velocity is a dipole in the particle distribution. If there is more angular structure then there will be higher moments of the distribution function. Typically the distribution is decomposed into spherical harmonics; for the photons this is equivalent to an angular distribution in temperature, with

$$T(\hat{\mathbf{r}}, \mathbf{x}, \eta) = \sum_{lm} T_{lm}(\mathbf{x}, \eta) Y_{lm}(\hat{\mathbf{r}}). \tag{52}$$

The T_{lm} moments are called multipoles, with $l = 0$ being the monopole, $l = 1$ being the dipole; we will discuss the harmonics in more detail later when we come to the CMB power spectrum.

Free streaming converts low multipoles to high multipoles as time evolves. To see this consider starting with a non-uniform (in space) temperature distribution, so there are hot and cold regions. Now if we turn off the scattering, photons can freely propagate. Initially if you are sitting in a hot spot you only see uniform hot photons coming from all directions, so still a monopole. But as the universe evolves you can see further away, so you start to see the nearby hot and cold spots: initially a small dipole in the distribution, then seeing structure on smaller scales as you see further away and hence more different hot and cold regions. So what started as a distribution with only the lowest multipoles ends up, after free streaming, with structure in lots of higher multipoles. This is why we see an anisotropy in the cosmic microwave background today, we're just seeing all the hot and cold spots on the last scattering surface when the universe recombined.

10. Photon diffusion: Silk damping

Fluctuations in the photons and baryons are damped by photon diffusion, baryons indirectly via their coupling to the photons prior to recombination. Photon perturbations smaller than the photon mean free path will be wiped out, but larger scales are also affected due to the photons random walking larger distances over multiple scattering events: the photons diffuse between hot and cold regions, dragging the tightly coupled baryons along with them, and hence smoothing out both distributions. This process is called *Silk damping*. The length scale is given by the random walk of photons before some relevant time, which we take to be recombination, η_*.

We can estimate an approximate result for Silk scale. At the epoch of interest the electrons are non-relativistic, and have much higher mass than the typical photon energy, so Compton scattering with photons is elastic. This is called Thomson scattering. If the density of free electrons is n_e, the scattering rate is $n_e\sigma_T$, where σ_T is the Thomson scattering cross-section (each photon scattering $n_e\sigma_T$ times per unit volume per unit time). The typical time between scatterings is therefore $\Delta t \sim 1/(n_e\sigma_T)$, or a comoving photon travel distance of $\Delta\eta \sim 1/(an_e\sigma_T)$. Taking random scattering directions $\hat{\mathbf{r}}_i$ to be independent, and using $n_e \approx n_H^0/a^3$ prior to recombination, we then expect a total diffusion length variance

$$\langle\eta_{\rm silk}^2\rangle \sim \left\langle\left(\sum_i(\Delta\eta)_i\hat{\mathbf{r}}_i\right)^2\right\rangle \sim \sum_{i,j}(\Delta\eta)_i(\Delta\eta)_j\langle\hat{\mathbf{r}}_i\hat{\mathbf{r}}_j\rangle \sim \sum_{i,j}(\Delta\eta)_i(\Delta\eta)_j\delta_{ij} \tag{53}$$

$$\sim \sum_i(\Delta\eta)_i^2 \sim \sum_i\frac{(\Delta\eta)_i}{an_e\sigma_T} \sim \int\frac{d\eta}{an_e\sigma_T} \sim \int\frac{a^2}{n_H^0\sigma_T}d\eta \sim \int\frac{\eta^4}{\eta_*^4}\frac{a_*^2}{n_H^0\sigma_T}d\eta \tag{54}$$

where n_e^0 is the number density of protons today. We approximated the background as matter domination until last scattering, so $a \propto \eta^2$. Integrating and calculating the rms gives

$$\eta_{\rm silk} \sim \sqrt{\frac{a_*^2\eta_*}{5n_H^0\sigma_T}} \sim 8{\rm Mpc}. \tag{55}$$

This is significantly smaller than the horizon size at recombination (as it must be!), so acoustic oscillations are only expected to be damped once they are well inside the horizon. See Fig. 1.

11. Free streaming of neutrinos and warm dark matter

Let's now consider the dark matter, which if it is not very cold may be made up of particles with a small velocity that can free stream but do not interact (no scattering). The comoving distance a free streaming particle can travel is

$$\int\frac{v(t)dt}{a} = \int v(\eta)d\eta, \tag{56}$$

so we expect dissipation on scales smaller than this: the particles rapidly move between regions of different density, wiping out density variations. Massless neutrinos free stream at the speed of light, since they are always decoupled after they freeze out. Initially neutrino density perturbations will start to collapse when they enter the horizon, just like photons, but because they can free-stream, they rapidly wash out and only have (small) acoustic oscillations to the extent that they are driven by the gravitational potentials generate by the photon (and matter) density perturbations.

Massive neutrinos will also free stream. In this case the total free-streaming length is the distance they travelled while relativistic (just the conformal time), plus the distance travelled once non-relativistic when the velocity redshifts approximately as $v \propto 1/a$:

$$r_\nu(\eta_0) \sim \eta_{nr} + \int_{\eta_{nr}}^{\eta_0} \frac{a_{rn}}{a} d\eta, \tag{57}$$

where nr denotes the time when they became non-relativistic. Current data suggest the neutrinos must be light enough to be relativistic at recombination, so we take η_{nr} to be during matter domination when $a \propto \eta^2$. Then

$$r_\nu(\eta_0) \sim \eta_{nr} + \int_{\eta_{nr}}^{\eta_0} \frac{\eta_{rn}^2}{\eta^2} d\eta = 2\eta_{nr} - \frac{\eta_{nr}^2}{\eta_0} \sim 2\eta_{nr}, \tag{58}$$

where we assume we are interested in the scale well after the neutrinos became non-relativistic. So scales $\gg \eta_{nr}$ are unaffected by the damping, but neutrino perturbations smaller than $2\eta_{nr}$ are suppressed. Of course neutrinos are only a small fraction of the matter density, so this has a correspondingly small (but potentially important) effect on the matter density.

If the dark matter itself has a small velocity dispersion, small enough that it becomes non-relativistic well before matter domination,

$$r_c(\eta_0) \sim \eta_{nr} + \int_{\eta_{nr}}^{\eta_{eq}} \frac{\eta_{nr}}{\eta} d\eta + \frac{\eta_{nr}}{\eta_{eq}} \int_{\eta_{eq}}^{\eta_0} \frac{\eta_{eq}^2}{\eta^2} d\eta = \eta_{nr} \left[2 + \ln\left(\frac{\eta_{eq}}{\eta_{nr}}\right) - \frac{\eta_{eq}}{\eta_0} \right], \tag{59}$$

where η_{eq} is the conformal time of matter-radiation equality ($\sim$ 120Mpc). A particle becomes non-relativistic when it's rest mass is comparable to its energy, so $m \sim k_B T_c(\eta_{nr})$. We just need to find T_c.

Now the ratio of the density of dark matter today is given by

$$\Omega_c = \frac{m n_{c0}}{\rho_{crit}} = \frac{\kappa m n_{c0}}{3H_0^2} = \kappa m \frac{n_{c0}}{n_{\gamma 0}} \frac{n_{\gamma 0}}{3H_0^2} = \kappa m \frac{n_c}{n_\gamma} \frac{n_{\gamma 0}}{3H_0^2} = \kappa m \left(\frac{T_c}{T_\gamma}\right)^3 \frac{n_{\gamma 0}}{3H_0^2} \tag{60}$$

where we used the constancy of $n_c/n_\gamma = n_{c0}/n_{\gamma 0}$ to relate the values today to those when the dark matter was relativistic. We assumed the dark matter had an equilibrium distribution with the same effective g^n as the photons when it was relativistic. The photon density today $n_{\gamma 0}$ is determined by standard results for a photon gas. Taking $H_0 = 100h\mathrm{kms}^{-1}\mathrm{Mpc}^{-1}$ and rearranging gives

$$T_c^3 \sim 0.026\, T_\gamma^3 \Omega_c h^2 \left(\frac{1\mathrm{keV}}{m}\right). \tag{61}$$

Setting $T_c \sim m/k_B$ for when the particles become non-relativistic with $T_\gamma \sim T_{\gamma 0}/a$ gives

$$\frac{m}{k_B} \sim \left(0.026 \Omega_c h^2 \frac{1\mathrm{keV}}{m}\right)^{1/3} \left(\frac{T_{\gamma 0}}{a_{nr}}\right), \tag{62}$$

which can be solved for a_{nr}. We just need to relate to η: using the radiation-dominated result $\mathcal{H}^2 = a^2 \kappa \rho_R/3 = \kappa \rho_{R0}/3a^2 = \Omega_R H_0^2/a^2$ we have

$$\eta = \mathcal{H}^{-1} = \frac{a}{\sqrt{\Omega_R H_0^2}} \tag{63}$$

to give

$$\eta_{nr} \sim 0.04\text{Mpc}\left(\Omega_c h^2\right)^{1/3}\left(\frac{1\text{keV}}{m}\right)^{4/3} \tag{64}$$

For $\Omega_c h^2 \sim 0.1$ and $m = 1$keV this implies a scale of about $r_c \sim 10\eta_{nr} \sim 0.2$Mpc. Warm dark matter with $m \sim$ keV would therefore be expected to form no structure on scales smaller than about 0.1Mpc. The presence of small-scale structure in the universe gives a constraint on how massive the dark matter particles must be, so we know $m \gtrsim 1$keV. If the mass is around this level it is called *warm dark matter*, if it is much larger so that free streaming effects are negligible it is called *cold dark matter*. Cold dark matter is always a good approximation on scales much larger than r_c as long as $P_c \ll \rho_c$. Currently there is no evidence the dark matter is warm.

IV. POWER SPECTRUM OF THE MATTER FLUCTUATIONS

We showed that inflation models predict a nearly scale-invariant spectrum of super-horizon curvature fluctuations. These are conserved through reheating, and hence give the initial conditions at the start of the radiation-dominated universe (hot big bang). A scale-invariant spectrum of curvature perturbations implies a scale-invariant spectrum of potential (Φ) fluctuations, which are related to the comoving total density perturbation by the Poisson equation. We now want to calculate what the density power spectrum will look like at later times, where it is more directly related to observations.

We can define a late-time power spectrum of the matter as before so that at a given time

$$\langle\Delta(\mathbf{x},t)^2\rangle = \int \frac{dk}{k}\mathcal{P}(k,t) \qquad \langle\Delta(\mathbf{k},t)\Delta(\mathbf{k}',t)\rangle = \frac{2\pi^2}{k^3}\mathcal{P}(k,t)\delta(\mathbf{k}+\mathbf{k}'). \tag{65}$$

For the matter power spectrum it is actually more conventional to define

$$P(k) \equiv \frac{2\pi^2}{k^3}\mathcal{P}(k), \tag{66}$$

in which definition a scale-invariant spectrum ($\mathcal{P} = \text{const}$) corresponds to $P(k) \propto 1/k^3$.

From the Poisson equation $\bar{\Delta} = -(2/3)k^2\Phi/\mathcal{H}^2$ we have

$$\mathcal{P}_{\bar{\Delta}}(\eta) \sim \frac{4}{9}\frac{k^4}{\mathcal{H}^4}\mathcal{P}_\Phi. \tag{67}$$

This is true on all scales. Since potentials are constant on all scales above the Jeans length during matter domination, the potential power spectrum for all modes that entered the horizon after matter domination ($k \ll \mathcal{H}_{eq}$) is a constant and proportional to the primordial power spectrum. The potential power spectrum when it was super-horizon can be obtained from the constant primordial comoving curvature perturbation using the result for matter domination that $\mathcal{R} = -\Phi + \Delta/(3+3w) = -\Phi + \Delta/3 = -\Phi - 2\Phi/3 = -5\Phi/3$ and hence $\mathcal{P}_\Phi = 9\mathcal{P}_\mathcal{R}/25$. Hence for scales with $k \ll \mathcal{H}_{eq}$, during matter domination

$$\mathcal{P}_{\bar{\Delta}}(\eta) \sim \frac{4}{9}\frac{k^4}{\mathcal{H}^4}\mathcal{P}_\Phi = \frac{4}{25}\frac{k^4}{\mathcal{H}^4}\mathcal{P}_\mathcal{R} \tag{68}$$

For a primordial spectrum $\mathcal{P}_\mathcal{R} \propto k^{n_s-1}$, the density power spectrum on these scales is $\mathcal{P}_{\bar{\Delta}} \propto k^{n_s+3}$. In terms of P we have $P_{\bar{\Delta}} \propto k^{n_s}$ (hence the otherwise odd conventional definition of n_s). Note $\mathcal{P}_\Phi$ is not actually constant when P/ρ varies (the change between radiation and matter domination is small, and it decays further when dark energy becomes important). However we saw in Eq. (25) that above the Jeans scale the matter perturbations evolve the same way independent of k, so the large-scale shape remains $\propto k^4$ times the primordial spectrum even after dark energy becomes important.

We now need to consider scales that entered the horizon before matter domination, when the potentials were not constant. Since $\bar{\Delta} = -(2/3)k^2\Phi/\mathcal{H}^2$, adiabatic perturbations in radiation domination have $\bar{\Delta}_c = 3\bar{\Delta}_\gamma/4 = 3\bar{\Delta}/4 = -(1/2)(k/\mathcal{H})^2\Phi$ until the perturbations come inside the horizon and

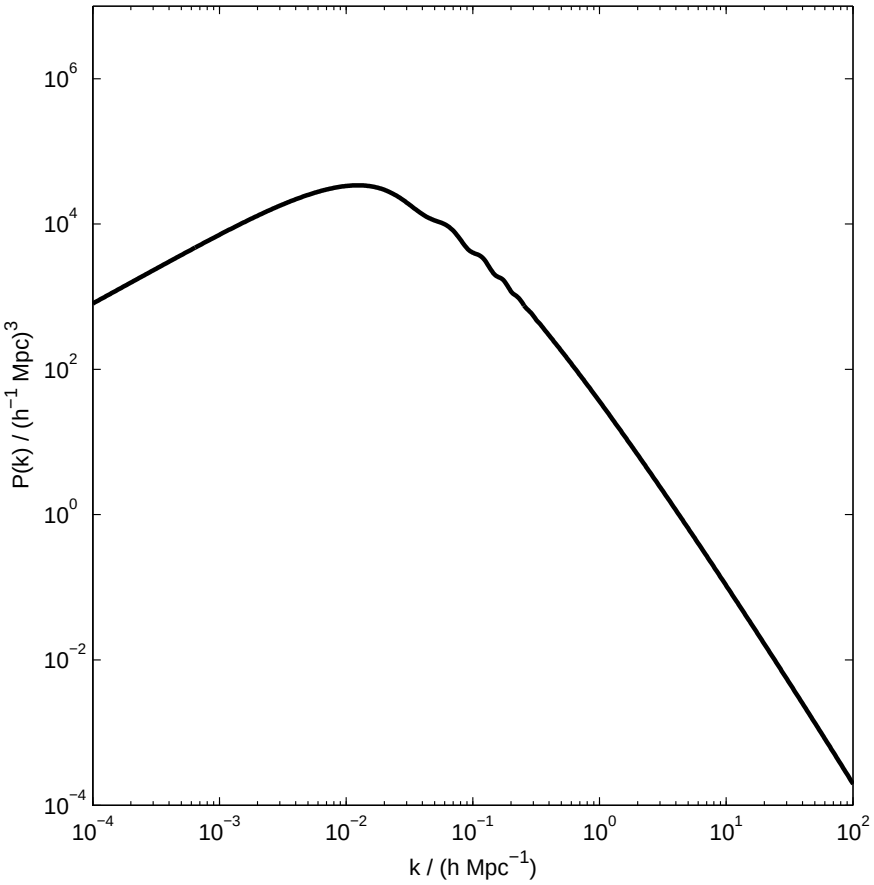

FIG. 3: The predicted linear power spectrum $P_{\bar{\Delta}}(k)$ for a cold dark matter model today ($z = 0$). On large scales $P \propto k^{n_s}$, on small scales $P \sim k^{4-n_s}$ with log growth. On intermediate scales the spectrum turns over and there are baryon oscillations on scales that were sub-horizon before recombination.

pressure support kicks in and the potentials fall to zero at $\eta_{\rm ln}$. The initial super-horizon conditions in radiation domination give $\mathcal{R} = -\Phi + \Delta/4 = -3\Phi/2$, and since $\mathcal{H} = 1/\eta$ we have[3] $\bar{\Delta}_c \sim (1/3)\mathcal{R}(k\eta)^2$ until logarithmic growth starts at $\eta_{\rm ln}$. After this the potentials have fallen to nearly zero and the matter perturbations grow only logarithmically until matter-radiation equality (Sec. II 4); thereafter during matter domination $\bar{\Delta} \sim \bar{\Delta}_c \propto a \propto \eta^2$, independent of scale. For $k \gg \mathcal{H}_{eq}$ and well after matter-radiation equality (but before dark energy is important) we therefore expect

$$\Delta_c(\eta) \sim \frac{1}{3}\mathcal{R}\,(k\eta_{\rm ln})^2\,[1 + 2\ln(\eta_{eq}/\eta_{\rm ln})]\left(\frac{\eta}{\eta_{eq}}\right)^2, \tag{69}$$

The coefficient of the log factor is chosen to keep the density and derivative continuous at $\eta_{\rm ln}$. We can take $\eta_{\rm ln} \sim 3\sqrt{3}\pi/(4k)$ as the time when logarithmic growth starts, and hence

$$\Delta_c(\eta) \sim \frac{9\pi^2}{16}\left[1 + 2\ln\left(\frac{4k\eta_{eq}}{\pi 3\sqrt{3}}\right)\right]\left(\frac{\eta}{\eta_{eq}}\right)^2 \mathcal{R} \tag{70}$$

---

[3] Note that in radiation domination the comoving gauge is not the rest frame of the dark matter, so $\bar{\Delta}_c$ and $\bar{\Delta}_\gamma$ are not the same as in the synchronous gauge.

and the power spectrum for $k \gg \mathcal{H}_{eq}$ at scale factor a during matter domination is

$$\mathcal{P}_{\bar{\Delta}} \sim \left(\frac{9\pi^2}{16}\right)^2 \frac{a^2}{a_{eq}^2}\left[1 + 2\ln\left(\frac{4k\eta_{eq}}{\pi 3\sqrt{3}}\right)\right]^2 \mathcal{P}_{\mathcal{R}}. \tag{71}$$

where $\mathcal{P}_{\mathcal{R}}$ is the initial value. The spectrum is close to scale-invariant; in terms of P we have $P_{\bar{\Delta}} \propto k^{n_s-4}$ with log corrections, though of course this is not accurate due to our various approximations. On intermediate scales the shape of the spectrum is continuous and depends on the details of the matter-radiation and recombination transitions. There are small wiggles (baryon oscillations) in the spectrum on scales below the horizon at recombination but above the Silk scale. Current observations suggest $\eta_{eq} \sim 120$Mpc, $z_{eq} = 1/a_{eq} - 1 \sim 3200$.

Once dark energy becomes important at late times the rate of growth slows, but the growth is still scale-independent. Also note that the potentials actually change slightly between matter and radiation domination.

If the dark matter is warm it will be wiped out on scales smaller than the free streaming length r_c. The baryons have non-zero pressure, which resists growth at the Jeans length, giving $\Delta_b \sim 3\Delta_c\mathcal{H}^2/(2k^2c_s^2)$ for $kc_s \gg \mathcal{H}$. At late times Δ becomes $\mathcal{O}(1)$ and linear theory breaks down. The perturbations then have to be evolved using N-body simulations, the results of which show that the power is boosted on small scales when non-linear growth can set it.

The exact form of the spectrum, for both hot and cold dark matter scenarios, can be found by numerical integration of the relevant equations. Popular numerical codes are called CMBFAST, CAMB (written by me, originally based on CMBFAST), CMBEASY, and CLASS, and work by evolving the multipoles of the distribution functions of the different stress-energy components using the perturbed Boltzmann equation. The details are beyond the scope of this course, but the results shown in Fig 3 and can be calculated numerically in about a second. Animations of how the transfer functions evolve with time can be seen at `http://cosmocoffee.info/viewtopic.php?t=1324`.

Since the dark matter is invisible, and we can only observe our past light cone not an entire spatial hypersurface, the matter power spectrum is not directly observable. However one can get quite close by observing the number density of galaxies: for Gaussian initial perturbations the power spectrum of the number density turns out on large-scales to be proportional to the matter power spectrum, and hence galaxies can indirectly be used to probe the matter power spectrum observationally.

V. COSMIC MICROWAVE BACKGROUND ANISOTROPIES

Recombination is a relatively sudden event at redshift $z \sim 1100$, so we can get a good qualitative handle on what we expect to see in the CMB anisotropies by considering all the CMB photons to come from a single nearly-spherical surface about us, where the universe suddenly transitions from being an opaque plasma to being mostly neutral hydrogen gas.

If we consider a photon propagating in a perturbed universe, integrating the geodesic equation for the conformal Newtonian gauge metric gives the energy today $E(\eta_0)$ in terms at the energy at a (conformal) time η (see the question sheet)

$$E(\eta_0) = a(\eta)E(\eta)\left[1 + \Psi(\eta) - \Psi_0 + \int_\eta^{\eta_0} d\eta(\Psi' + \Phi')\right], \tag{72}$$

to linear order in the perturbations. Here the integral is along the photon path; since the integrand is already first order, the integral can be taken to be along the unperturbed (background, zeroth order) photon path. What we mean by "along the photon path" is that in the integrand Ψ and Φ are evaluated at the position the photon had at time η, i.e. $\Phi(\mathbf{x}, \eta) = \Phi(\mathbf{x}_0 + (\eta_0 - \eta)\hat{\mathbf{n}}, \eta)$ where $\mathbf{x}_0$ is the location of the observer and $\hat{\mathbf{n}}$ is the unit vector in the direction in which we are observing the photon. The energies are those observed by an observer with no peculiar velocity.

At zeroth order this equation agrees with the FRW result, that $E \propto E_0/a$. The corrections in the perturbed universe are due to the difference in potentials between the point of emission and reception, $\Psi(\eta) - \Psi_0$ (the net red/blue shift as the photon climbs out/falls into the potential wells at the two points), and an integrated contribution which is call the Integrated Sachs-Wolfe (ISW) effect. This reflects the net blue/red-shift as the photon falls into and falls out of the evolving potentials along the

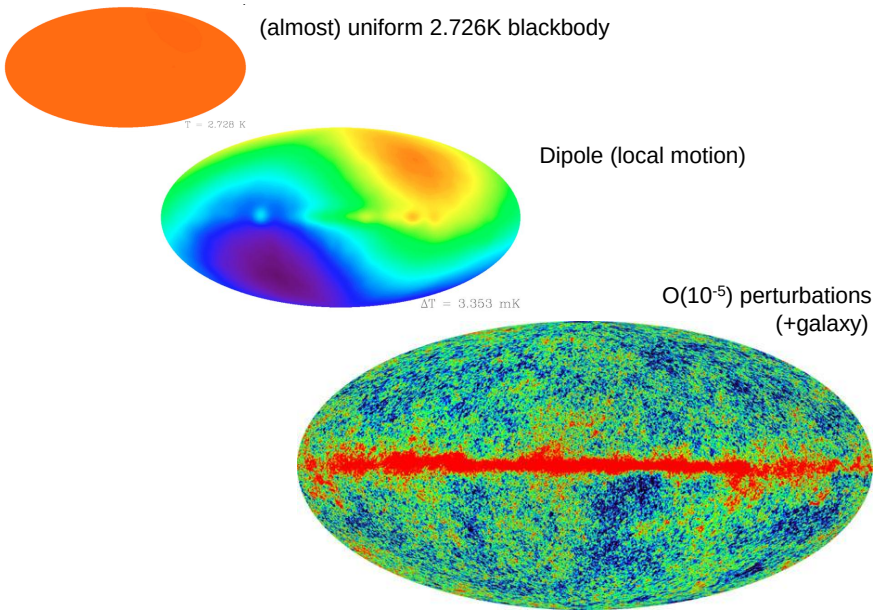

FIG. 4: The observed CMB sky: almost uniform, with the monopole subtracted showing the $\mathcal{O}(10^{-3})$ dipole due to local motion, and with both the monopole and dipole subtracted to show the anisotropies (+ foreground contamination from our galaxy).

line of sight. In a matter dominated universe $\Phi' = \Psi' = 0$, so this term vanishes: there is an exact cancellation between the blue and red shifts as the photon falls into and climbs out of the potentials. However since there is dark energy at late time, this term is not zero, with the contribution from $z \lesssim 1$ when dark energy becomes important being called the "late-time integrated Sachs-Wolfe effect". For the CMB, where photons decoupled at recombination, there is also some evolution of the potentials near the start of the photon paths because recombination was not completely matter-dominated (there was still some contribution to the energy density from radiation).

The energies above are when there are no peculiar velocities, $E = p^\nu u_\nu$ where u^ν is the four-velocity of a source/observer at rest in the Newtonian gauge. If the source velocity is $u_s^\nu = u^\nu + v^\nu$, and $p^\nu = E(u^\nu + e^\nu)$ (so the photon is moving towards us in spatial direction e^ν, with $e^\nu u_\nu = 0$, $e^\nu e_\nu = -1$), the energy in the source rest frame is $E_s = u_s^\nu p_\nu = E(1 + v^\nu e_\nu)$ at first order. Since the photon is moving towards us, in direction $\hat{\mathbf{n}}$ we have $\mathbf{e} = -\hat{\mathbf{n}}$, so $E_s = E(1+\mathbf{v}\cdot\hat{\mathbf{n}})$. If we also have some peculiar velocity $\mathbf{v}_{\rm obs}$ (as we do), the observed energy is similarly $E_{\rm obs} = u_{\rm obs}^\nu p_\nu = E_0(1 + \mathbf{v}_{\rm obs}\cdot\hat{\mathbf{n}})$. Accounting for peculiar velocities the observed energy and source rest-frame energy are related by

$$\begin{aligned} E_{\rm obs} &= a(\eta)\frac{E_s(\eta)}{1+\mathbf{v}\cdot\hat{\mathbf{n}}}\left[1+\Psi(\eta)-\Psi_0+\int_\eta^{\eta_0} d\eta(\Psi'+\Phi')\right](1+\mathbf{v}_{\rm obs}\cdot\hat{\mathbf{n}}) \\ &= a(\eta)E_s(\eta)\left[1+\Psi(\eta)-\Psi_0+\hat{\mathbf{n}}\cdot(\mathbf{v}_{\rm obs}-\mathbf{v})+\int_\eta^{\eta_0} d\eta(\Psi'+\Phi')\right] \end{aligned} \tag{73}$$

Since CMB photons last scattered from electrons (which are very tightly coupled to the baryons), the relevant source rest frame is that of the baryons, so the relevant source velocity is $\mathbf{v}_b$.

Photons of all frequencies redshift in the same way because $E_{\rm obs}/E_s(\eta)$ is independent of E. A redshift in each photon energy therefore directly corresponds to a redshift in the observed CMB temperature: we can define $T_{\rm obs}$ with $T_{\rm obs}/T_s(\eta) = E_{\rm obs}/E_s(\eta)$, and the photon energy distribution remains blackbody if it was at recombination. However because the times at which photons recombined can be different in different directions on the sky, the temperature that we observe in the perturbed universe is not isotropic.

In Eq. (73) we have given the result for the change in energy between two conformal times. What conformal time do we need for the CMB? Recombination is governed by the temperature of the photon-baryon plasma, so we are seeing photons coming from a nearly-spherical surface about us, where each point in the surface has the same temperature at which recombination happens $T_s(\eta) = T_*$. This will be at a different distance (and hence conformal time) from us in different directions, since for example hotter regions will recombine later. If we define η_* as being the conformal time of recombination in the background FRW universe, then in any given direction photons will be coming from a perturbed time $\eta = \eta_* + \delta\eta$ with $a(\eta) = a_* + \delta a$ (where $\delta a/a = \mathcal{H}\delta\eta$).

So the observed temperature in a direction $\hat{\mathbf{n}}$ is

$$\begin{aligned} T_{\rm obs}(\hat{\mathbf{n}}, \eta_0) &= (a_* + \delta a)T_* \left[1 + \Psi(\eta_*) - \Psi_0 + \hat{\mathbf{n}}\cdot(\mathbf{v}_{\rm obs} - \mathbf{v}) + \int_{\eta_*}^{\eta_0} d\eta(\Psi' + \Phi')\right], \\ &= T_0 \left[1 + \frac{\delta a}{a_*} + \Psi(\eta_*) - \Psi_0 + \hat{\mathbf{n}}\cdot(\mathbf{v}_{\rm obs} - \mathbf{v}) + \int_{\eta_*}^{\eta_0} d\eta(\Psi' + \Phi')\right] \end{aligned} \tag{74}$$

where the background CMB temperature today is $T_0 = T_* a_*$. Note that $\Psi(\eta) = \Psi(\eta_*)$ to first order, and similarly the limits of the integral can also be taken to be the background values at first order.

Since the photons have a blackbody spectrum, and recombination is a fixed temperature surface, $\rho_\gamma(\eta, \mathbf{x}) = \rho_{\gamma *} = a_R T_*^4$. Since $\rho_\gamma(\eta, \mathbf{x}) = \rho_{\gamma *} + \rho'_\gamma \delta\eta + \delta\rho_\gamma = \rho_{\gamma *}$, the change in density due to the delay in recombination has to be cancelled by the density perturbation, $\delta\eta = -\delta\rho_\gamma/\rho'_\gamma = \Delta_\gamma/(4\mathcal{H})$ (i.e. to cool to the recombination temperature, an overdensity has to expand for longer). So the perturbation to the scale factor is $\delta a/a = \Delta_\gamma/4$. This can also be seen directly from $\rho_\gamma \propto T^4 \propto a^4$, so $\delta a/a = \delta T/T = \Delta_\gamma/4$. Hence we can write the observed fractional temperature anisotropy as

$$\frac{\Delta T_{\rm obs}}{T}(\hat{\mathbf{n}}) = \frac{\Delta_\gamma}{4} + \Psi - \Psi_0 + \hat{\mathbf{n}}\cdot(\mathbf{v}_{\rm obs} - \mathbf{v}) + \int_{\eta_*}^{\eta_0} d\eta(\Psi' + \Phi') \tag{75}$$

where terms on the RHS are evaluated at time η_* at the spatial position corresponding to the background photon path at time η_*. Remember that we are using the CNG, and since on large scales perturbations will be super-horizon sized at recombination, the distinction between CNG and other gauges can be important.

From Eq. (46) on super-horizon modes $\bar{\Delta} = \Delta + 2\Phi$ if the equation of state is constant. In the approximation in which recombination is matter dominated, and the perturbations are adiabatic so $\Delta = \Delta_m = 3\Delta_\gamma/4$, on super-horizon scales we have $\Delta \to \Delta_m = 3\Delta_\gamma/4 \to -2\Phi = -2\Psi$. So in the large-scale limit the source term $\Delta_\gamma/4 + \Psi \to -2\Psi/3 + \Psi = \Psi/3$: this is the Sachs-Wolfe contribution to the large-scale CMB anisotropy in the matter-dominated approximation.

On sub-horizon scales $|\bar{\Delta}_\gamma| \gg |\Psi|$ (from the Poisson equation), so the density perturbation $\Delta_\gamma \approx \bar{\Delta}_\gamma$ dominates the contributions to the CMB anisotropy. So small hotspots on the CMB correspond to hot overdensities at last scattering: the photons from these hot patches have seen less change in scale factor between the source and observation, and so have been less redshifted, and hence appear hotter. Sources from underdensities recombined earlier, had a larger redshift, and so appear colder. On the other hand for a super-horizon-sized overdensity this is different: the large-scale anisotropy is dominated by the redshift of the photon as it climbed out of the potential well at last scattering, and hence appears cold on the sky today. Large-scale overdensities look cold, small scale overdensities look hot (and vice versa for underdensities).

The velocities (doppler terms) are important on scales where the acoustic oscillations are mid-oscillation at recombination, so that density perturbation is small but the velocities are largest. They ensure that there is a significant variance to the anisotropy on all scales, rather going to zero. The local doppler term is also important as it gives rise to a large dipole in the observed CMB temperature which must be subtracted to get at the $\mathcal{O}(10^{-5})$ anisotropies from recombination.

A. Beyond a single scattering surface

In reality recombination is not completely sudden, and the ionization fraction x_e takes an appreciable time to change from being $x_e \sim 1$ to being nearly neutral with $x_e \sim 0$. In terms of comoving distance, from the hot big bang till recombination is around 300Mpc, and the thickness of the recombination surface is roughly 100Mpc. This has several important consequences:

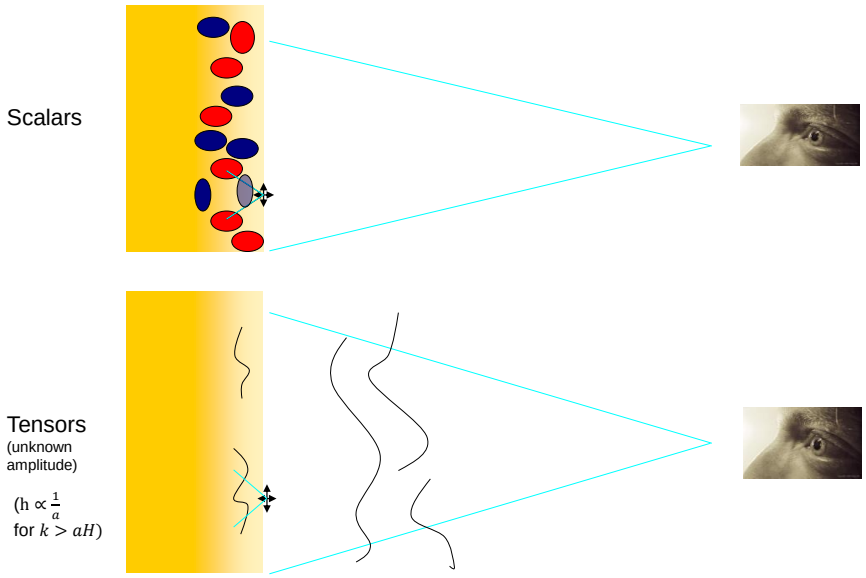

FIG. 5: An illustration (not to scale!) of how we view the last scattering surface and the sources of density and tensor anisotropies.

- When we look at a given point on the last scattering surface, we are actually seeing a mixture of photons coming from different times during recombination, meaning that we are effectively measuring an averaged version of the previous result. The function $g(\eta)$ which gives the probability that a given photon came from a shell at time η is called the *visibility*. First let's define $P(\eta)$ as the probability that a photon travels freely from time η until today (without scattering). The probability of a photon Thomson scattering in a time $d\eta$ is $an_e\sigma_T d\eta$, so the probability of not having scattered from an earlier time $\eta - d\eta$ is $P(\eta - d\eta) = P(\eta)(1 - an_e\sigma_T d\eta)$. Expanding in $d\eta$ then gives

$$-\frac{dP}{d\eta}d\eta = -an_e\sigma_T P d\eta \implies \frac{1}{P}\frac{dP}{d\eta} = an_e\sigma_T \implies \ln P = -\int_\eta^{\eta_0} an_e\sigma_T d\eta'.$$

  Hence $P = e^{-\tau}$ where we have defined the optical depth between time η and today to be

$$\tau \equiv \int_\eta^{\eta_0} an_e\sigma_T d\eta'.$$

  The factor $e^{-\tau}$ is the fraction of photons from time η that we actually receive rather than being scattered. The visibility is then determined by $dP = g(\eta)d\eta$ being the number of photons last-scattering at time η in interval $d\eta$, and hence

$$g = \frac{dP}{d\eta} = -\tau' e^{-\tau}.$$

  This is fairly sharply peaked at recombination as we expect, but has some finite thickness. The anisotropies we observe are then the weighted integral $\int d\eta g(\eta)$ of our previous result. In particular this means that small-scale perturbations get averaged out: if there is a hot and cold spot along the line of sight through the last-scattering surface, we will observe some average. This reduces the amplitude of the fluctuations we observe on scales smaller than the thickness of the last-scattering surface. See the schematic top of Fig. 5.

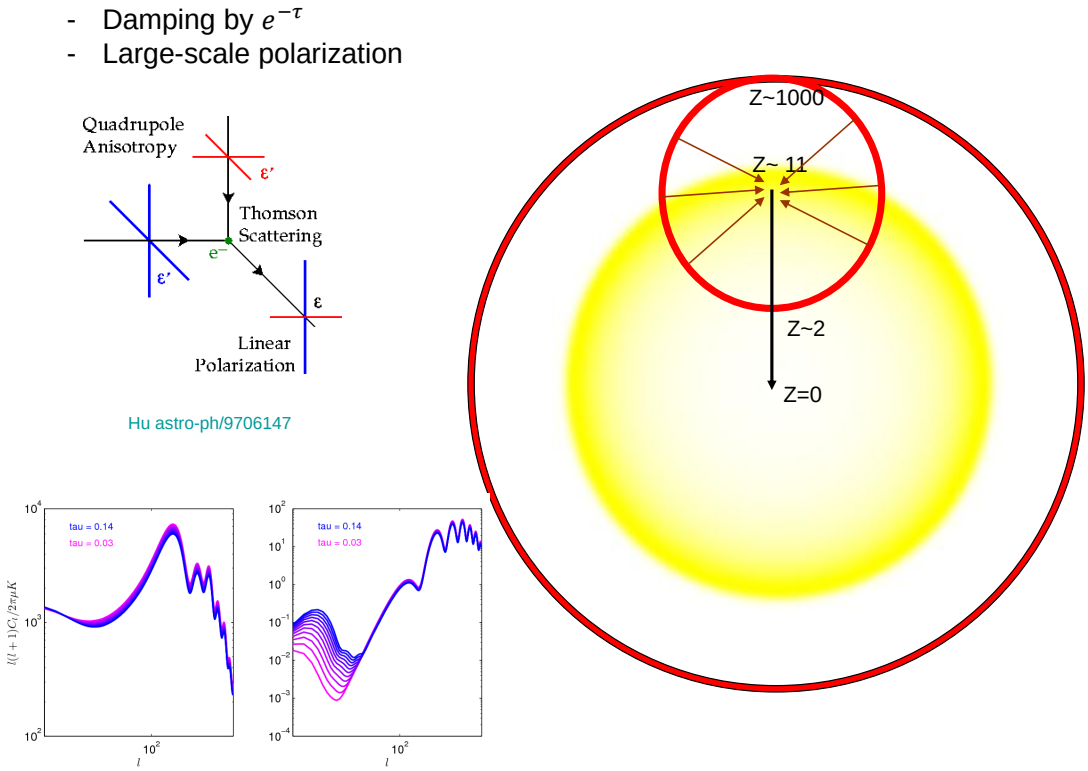

FIG. 6: An illustration of the source of polarization from Thomson scattering at reionization. The lower left plots show the effect on the CMB power spectra as a function of optical depth (temperature power spectrum on the left is just damped on small scales, E-mode polarization on the right has an additional large-scale bump from scattering at reionization. The diagram on the right is of the observable universe in comoving distance, with the yellow shading showing the visibility during reionization (most of the scattering at reionization happens around $z \sim 11$, at later times the electron density dilutes due to the expansion so scattering is less likely).

- We previously described the effect of Silk Damping: photon diffusion leads to very small scale fluctuations being entirely erased.
- An electron towards the end of recombination with be able to partly see nearby hot and cold spots: the distribution of photons arriving at the electron will be anisotropic. If there is a quadrupole component to the photon distribution, the scattered light has a linear polarization. This leads to the CMB being polarized at around the 10% level, so observations of the polarization can be used to learn more information about the early universe in addition to the temperature anisotropy. An accurate calculation of the temperature perturbations also has to account for the anisotropy in the photon scattering; numerical codes work by integrating the full perturbed Boltzmann equation and include anisotropic source terms in the line-of-sight integral. See Fig. 6.

After recombination most of the photons do travel without further scattering until we observe them. However somewhere around redshift $z \sim 11$ the universe actually reionized, as energetic photons from the first stars and quasars caused the neutral hydrogen to become ionized again. Since the universe has greatly expanded between redshift $z \sim 1100$ and $z \sim 11$, the number density of electrons is now much lower, so most of the photons do not scatter even though the universe becomes fully ionized again. However some number do scatter, and the optical depth of reionization is found to be around $\tau \sim 0.1$, so around 10% of the photons from recombination are re-scattered at reionization. This leads

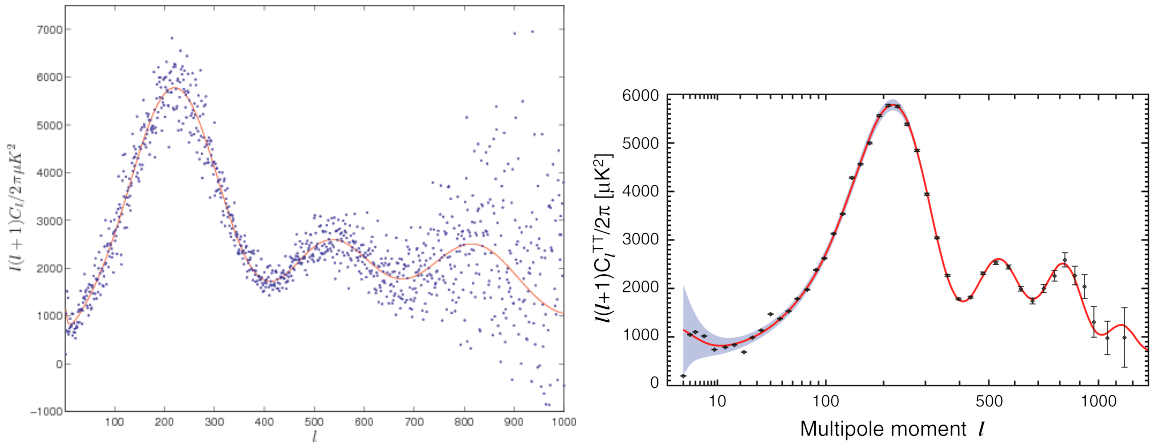

FIG. 7: Left: The $\hat{C}_l$ measured by WMAP (7 years, the blue points), and the best-fit theoretical power spectrum C_l. For $l \lesssim 400$ the points are scattered just by cosmic variance, on smaller scales there is additional scatter due to observational noise. Right: the same data after the points have been binned to reduce the scatter.

to a $e^{-\tau}$ suppression of the small-scale anisotropies (small-scale being smaller than the horizon-size at reionization). More interestingly the free electrons from reionization will see an anisotropic photon distribution and hence produce polarization by Thomson scattering. This gives rise to a large-scale polarization signal that is much larger than the polarization signal from recombination on those scales $l \lesssim 20$.

B. The CMB power spectrum

Since all the linear perturbations are expected to be nearly Gaussian, and the temperature anisotropy is just a linear combination of linear sources, the CMB is also expected to be nearly Gaussian. It should also be statistically isotropic from the assumed underlying statistical homogeneity and isotropy of the model. Gaussian fluctuations about the mean are entirely characterized by their variance. In the case of the matter density we defined the matter power spectrum to quantify the variance of the fluctuations a function of scale, encoded in the wavevector k from a spatial Fourier transform. For the CMB we can only observe the anisotropy as a function of direction, so the observation can be thought of as being on the surface of a sphere (corresponding to us looking at the last-scattering surface in all directions). In this case the eigenfunctions of the Laplacian on the sphere are the spherical harmonics Y_{lm}, with $\nabla^2 Y_{lm} = -l(l+1)Y_{lm}$, so we instead expand the data in spherical harmonics with

$$T(\hat{\mathbf{n}}) = \sum_{lm} T_{lm} Y_{lm}(\hat{\mathbf{n}}) \tag{76}$$

$$T_{lm} = \int d\Omega_{\hat{\mathbf{n}}} T(\hat{\mathbf{n}}) Y_{lm}(\hat{\mathbf{n}})^*. \tag{77}$$

The l index quantifies the scale, as k did in 3-D space, with low l corresponding to long-wavelength modes. The index m satisfies $-l \leq m \leq l$, so there are $2l+1$ different m values for each l, corresponding to different $e^{im\phi}$ modes. The lowest mode $l = 0$ corresponds to the monopole, the uniform component of the observed temperature (the average). The $l = 1$ modes correspond to a dipole pattern, and the m values correspond to the three numbers required to specify the direction and magnitude of the dipole. The Sachs-Wolfe result for the CMB applies at $l \lesssim 100$ where perturbations were super-horizon at recombination.

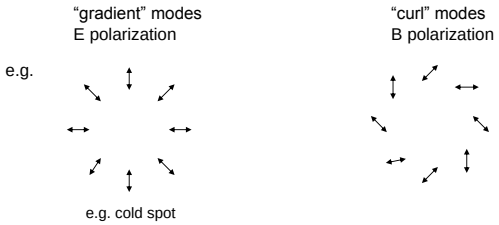

FIG. 8: Examples of E and B mode patterns of CMB polarization

The CMB power spectrum is then defined to quantify the variance in the T_{lm} as a function of l, with

$$C_l \equiv \langle |T_{lm}|^2 \rangle. \tag{78}$$

For a statistically isotropic distribution the power spectrum is only a function of l not m, and $\langle T_{lm} T^*_{l',m'} \rangle = \delta_{ll'}\delta_{mm'}C_l$. If the temperature on the sky is measured, in terms of the observed T_{lm} one can estimate the power spectrum using

$$\hat{C}_l = \frac{1}{2l+1}\sum_m |T_{lm}|^2, \tag{79}$$

where the expectation value give the true power spectrum, $\langle \hat{C}_l \rangle = C_l$. It is important to distinguish between $\hat{C}_l$ and C_l: the latter is the average value of $\hat{C}_l$ if one could observe an infinite ensemble of universes. In our own universe we can only observe $\hat{C}_l$, which differs from C_l by *cosmic variance* (see Fig. 7). Explicitly, the variance of $\hat{C}_l$ is given by

$$\begin{aligned} \mathrm{var}(\hat{C}_l) &= \left\langle \left(\hat{C}_l - C_l\right)^2 \right\rangle \\ &= \frac{1}{(2l+1)^2}\sum_{mm'} \langle |T_{lm}|^2 |T_{lm'}|^2 \rangle - 2\langle \hat{C} \rangle C_l + C_l^2 \\ &= \frac{1}{(2l+1)^2}\sum_{mm'} \left(C_l^2 + \delta_{mm'} 2C_l^2\right) - C_l^2 = \frac{2C_l^2}{2l+1}. \end{aligned} \tag{80}$$

So from an observation of $\hat{C}_l$ we can only say (roughly) that $C_l = \hat{C}_l \pm \sqrt{2/(2l+1)}\hat{C}_l$. For low l (large-scales), this significantly restricts the precision with which we can measure C_l, an unavoidable consequence of only having access to observations from one position in one universe.

C. Gravitational waves

So far we have only discussed the anisotropies cause by scalar perturbations. However there may also be primordial gravitational waves, which could give rise to an observable signal in the CMB that can be used to constrain the model of inflation.

Gravitation waves decay $\propto 1/a$ once they enter the horizon, so any waves that entered the horizon well before recombination have no effect on the CMB. However modes entering the horizon between last-scattering and today can anisotropically redshift the background CMB at recombination, giving rise to additional temperature anisotropies on large scales $l \lesssim 200$. Modes entering the horizon during the process of recombination can also induce a quadrupole towards the end of recombination, and

hence give rise to CMB polarization (see lower schematic in Fig. 5). In addition the waves entering the horizon between recombination and reionization will generate a quadrupole at reionization, and hence give rise to a large-scale polarization signal from Thomson scattering at reionization.

Cosmic variance limits our ability to tell if the large-scale temperature has a small additional component from gravitational waves. However the polarization signal is more distinctive: there are two distinct type of polarization patterns that can be observed, gradient-type *E mode* polarization, and curl-type *B mode* polarization (see Fig. 8). The E mode patterns are what we expect to see from scalar perturbations, for example a radial polarization pattern around the hot and cold spots. However the B mode patterns have a handedness to them that cannot be generated by purely scalar perturbations at linear order (however they can be produced at a low level at higher order by gravitational lensing of E modes). So if we can observe B modes, they are a 'smoking gun' of gravitational waves, at least for $r \gtrsim 0.001$ where they are at a level that's larger than that from gravitational lensing of scalar modes.

Although we only discussed the temperature harmonics and power spectrum in the previous section, analogous but more complicated spherical harmonic transforms can be defined for the polarization, giving E_{lm} and B_{lm} modes that also define angular power spectra C_l^{EE} and C_l^{BB} as for the temperature.

D. Calculating the temperature power spectrum

The power spectrum is the variance of the angular multipoles on the sky, so to calculate the power spectrum we need to relate this to fourier modes in the volume that is being observed. This is done using the Rayleigh plane-wave expansion:

$$e^{i\mathbf{k}\cdot\mathbf{x}} = 4\pi \sum_{lm} i^l j_l(kx) Y^*_{lm}(\hat{\mathbf{k}}) Y_{lm}(\hat{\mathbf{x}}), \tag{81}$$

where $j_l(x)$ is a *spherical Bessel function*. Let's consider just the scalar part of the temperature anisotropy source from recombination, $S \equiv \frac{\Delta_\gamma}{4} + \Psi$, in the approximation of instantaneous recombination. Recall that in linear theory we can define a transfer function $T_S(\eta, k)$ so that $S(\eta, \mathbf{k}) = T_S(\eta, k)\mathcal{R}(0, \mathbf{k})$ where $\mathcal{R}(0, \mathbf{k})$ is the Fourier mode of the super-horizon curvature perturbation at the start of the hot big bang. Then

$$\begin{aligned} \frac{\Delta T_{\rm obs}}{T}(\hat{\mathbf{n}}) &= \int \frac{d^3\mathbf{k}}{(2\pi)^{3/2}} S(\eta_*, \mathbf{k}) e^{i\chi_* \mathbf{k}\cdot\hat{\mathbf{n}}} \\ &= 4\pi \int \frac{d^3\mathbf{k}}{(2\pi)^{3/2}} T_S(\eta_*, k)\mathcal{R}(0, \mathbf{k}) \sum_{lm} i^l j_l(k\chi_*) Y^*_{lm}(\hat{\mathbf{k}}) Y_{lm}(\hat{\mathbf{n}}) \end{aligned} \tag{82}$$

where $\chi_* = \eta_0 - \eta_*$ is the comoving radial distance to the last-scattering surface. From this we can read off the harmonic components of $\frac{\Delta T_{\rm obs}}{T}(\hat{\mathbf{n}}) = \sum_{lm} a_{lm} Y_{lm}(\hat{\mathbf{n}})$ giving

$$a_{lm} = 4\pi i^l \int \frac{d^3\mathbf{k}}{(2\pi)^{3/2}} T_S(\eta_*, k)\mathcal{R}(0, \mathbf{k}) j_l(k\chi_*) Y^*_{lm}(\hat{\mathbf{k}}). \tag{83}$$

We can now calculate the power spectrum by using the definition of the primordial power spectrum $\langle \mathcal{R}(0, \mathbf{k})\mathcal{R}(0, \mathbf{k}')\rangle = (2\pi^2/k^3)\mathcal{P}_\mathcal{R}(k)\delta(\mathbf{k} + \mathbf{k}')$ giving

$$\begin{aligned} &\langle a_{lm} a^*_{l'm'}\rangle = \\ &(4\pi)^2 i^{l-l'} \int \frac{d^3\mathbf{k}}{(2\pi)^{3/2}} \int \frac{d^3\mathbf{k}'}{(2\pi)^{3/2}} T_S(\eta_*, k) T_S(\eta_*, k') \langle \mathcal{R}(0, \mathbf{k})\mathcal{R}(0, \mathbf{k}')^*\rangle j_l(k\chi_*) j_{l'}(k'\chi_*) Y^*_{lm}(\hat{\mathbf{k}}) Y_{l'm'}(\hat{\mathbf{k}}') \\ &\quad = (4\pi)^2 i^{l-l'} \int \frac{d^3\mathbf{k}}{(2\pi)^3} \frac{2\pi^2 \mathcal{P}_\mathcal{R}(k)}{k^3} j_l(k\chi_*) j_{l'}(k\chi_*) [T_S(\eta_*, k)]^2 Y_{lm}(\hat{\mathbf{k}})^* Y_{l'm'}(\hat{\mathbf{k}}) \\ &\quad = 4\pi \delta_{ll'} \delta_{mm'} \int d\ln k \mathcal{P}_\mathcal{R}(k) [T_S(\eta_*, k) j_l(k\chi_*)]^2, \end{aligned}$$

where in the last like we used orthogonality of the spherical harmonics, $\int d\Omega Y_{lm} Y^*_{l'm'} = \delta_{ll'}\delta_{mm'}$, showing that as expected for a statistically isotropic ensemble the different a_{lm} are uncorrelated to each other. Hence the power spectrum is given by

$$C_l \;=\; 4\pi \int d\ln k \mathcal{P}_\mathcal{R}(k)[T_S(\eta_*,k) j_l(k\chi_*)]^2. \tag{84}$$

If we consider very large scales and approximate recombination as matter dominated, $\mathcal{R} = -\Phi + \Delta/(3+3w) = -\Phi + \Delta/3 = -\Phi - 2\Phi/3 = -5\Phi/3$ is constant on super-horizon scales. In this case $S = \Phi/3 = -\mathcal{R}/5$ and hence $T_S(\eta_*,k) = -1/5$. The power spectrum is then approximately

$$C_l \approx \frac{4\pi}{25} \int d\ln k \mathcal{P}_\mathcal{R}(k)[j_l(k\chi_*)]^2. \tag{85}$$

If the primordial spectrum is exactly scale-invariant $\mathcal{P}_\mathcal{R}(k) = A_s$ is independent of k, and

$$\begin{aligned} C_l \quad &\approx \quad A_s \frac{4\pi}{25} \int d\ln k [j_l(k\chi_*)]^2 = A_s \frac{4\pi}{25} \frac{1}{2l(l+1)} \\ &\implies \quad \frac{l(l+1)C_l}{2\pi} = \frac{A_s}{25}, \end{aligned} \tag{86}$$

which is a scale-invariant power spectrum. People usually plot the power spectrum as $\frac{l(l+1)C_l}{2\pi}$ so that a constant value is scale-invariant, and the total variance of the anisotropies at any point (the same in all directions, by statistical isotropy) is given by

$$\begin{aligned} \langle \left(\frac{\Delta T}{T}\right)^2 \rangle \;&=\; \sum_{lm} C_l Y_{lm} Y^*_{lm} = \sum_{lm} C_l \frac{1}{4\pi} \int d\Omega Y_{lm} Y^*_{lm} = \sum_{lm} \frac{C_l}{4\pi} = \sum_l \frac{2l+1}{4\pi} C_l \\ &\approx \; \int d\ln l \frac{l(l+1)C_l}{2\pi}. \end{aligned} \tag{87}$$

Hence $\frac{l(l+1)C_l}{2\pi}$ is also roughly the variance per $\log l$, and the area under a plot of $\frac{l(l+1)C_l}{2\pi}$ against $\ln l$ is just the total variance.

On smaller scales the $\Delta_\gamma/4$ source term becomes important. We showed in Sec. II 3 that the radiation density undergoes acoustic oscillations on sub-horizon scales, as the fluid falls into potential wells, becomes pressure supported and bounces in and out. At the time of recombination this means that $\Delta_\gamma/4$ oscillates in k, which translates into an oscillation in l, with $k\chi_* \sim l$ (the spherical Bessel functions peak around $l \sim k\chi_*$). This gives rise to the acoustic oscillations in the C_l, naively $\sim \cos^2(k\eta_*/\sqrt{3}) \sim \cos^2(l\eta_*/[\sqrt{3}\chi_*])$. In reality the power does not pass through zero because of the additional doppler contributions (which are largest when $\Delta_\gamma \sim 0$ as the fluid is flowing most rapidly in or out of a potential well), and the speed of sound is less than $1/\sqrt{3}$ due to the inertia of the tightly-coupled baryons. The power spectrum also falls on small scales due to line-of-sight averaging and Silk damping. On large-scales the power spectrum is approximately flat, but there is an additional contribution from the ISW effect from photons falling in and out of potential wells after dark energy has become important.

The presence of baryons also makes the gravitational wells deeper when the baryon-photon fluid falls into an overdensity, making the gas compress even more. On the other hand when the acoustic oscillations are at the point where the overdensities are rarefied, there the baryons do not act to make it more rarefied. This leads to a difference in the amplitude of the compression and rarefaction peaks of the density oscillations (i.e. the odd and even peaks of the power spectrum). By comparing the amplitudes it is possible to estimate the amount of baryons in the universe. The results are consistent with those from big-bang nucleosynthesis.

As with the matter power spectrum, accurate numerical predictions for the C_l given the various cosmological parameters can be calculated easily using standard numerical codes like CMBfast, CAMB and CMBeasy in around a second. Even much more detailed analytical treatments than we have given here struggle to get close to percent-level accuracy, and current observations such as Planck are already sensitive enough to measure smooth changes in the C_l of order 0.3%, so a full numerical calculation is essential. The main contributions to the full numerical result are shown in Fig. 9.

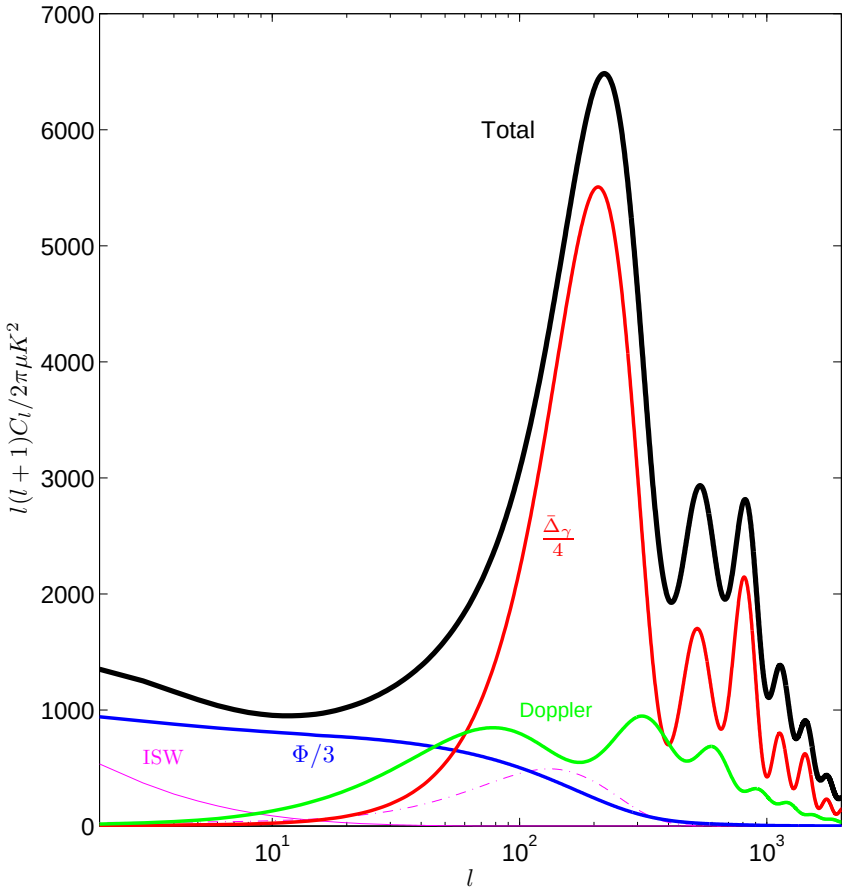

FIG. 9: Power spectrum of the contributions to the total CMB temperature anisotropy C_l. The red $\bar{\Delta}_\gamma$ contribution is the main small-scale contribution from the comoving temperature perturbations at last-scattering, with $\Phi/3$ being the large-scale contribution from photons climbing out of potential wells. Note that the $\Phi/3$ and $\bar{\Delta}_\gamma$ source terms have opposite sign, to their total contribution to the power spectrum is nearly zero at $l \sim 60$, where the total is then dominated by the doppler term. The magenta ISW contributions come from the late-time change in the potentials when dark energy becomes important at low redshift (solid), and the early contribution (dash-dotted) from time-varying potentials soon after recombination as the universe became fully matter rather than radiation dominated.